Science of the Total Environment 666 (2019) 126–138

Contents lists available at ScienceDirect

Science of the Total Environment

journal homepage: www.elsevier.com/locate/scitotenv

Climate-associated rice yield change in the Northeast China Plain: A simulation analysis based on CMIP5 multi-model ensemble projection

He Zhang [a], Guangsheng Zhou [a,*], De Li Liu [b,c], Bin Wang [b], Dengpan Xiao [d], Liang He [e]

[a] State Key Laboratory of Severe Weather, Chinese Academy of Meteorological Sciences, Beijing 100081, China
[b] NSW Department of Primary Industries, Wagga Wagga Agricultural Institute, Wagga Wagga, NSW 2650, Australia
[c] Climate Change Research Centre and ARC Centre of Excellence for Climate Extremes, University of New South Wales, Sydney, NSW 2052, Australia
[d] Institute of Geographical Sciences, Hebei Academy of Sciences, Shijiazhuang 050011, China
[e] National Meteorological Center, Beijing 100081, China

HIGHLIGHTS

- The future climate will have positive impacts on rice yields in Northeast China.
- Increased radiation and elevated CO_2 concentration are the main reason for future rice yield increase in Northeast China.
- High latitude areas have a large yield increase than the low latitude regions in Northeast China.

GRAPHICAL ABSTRACT

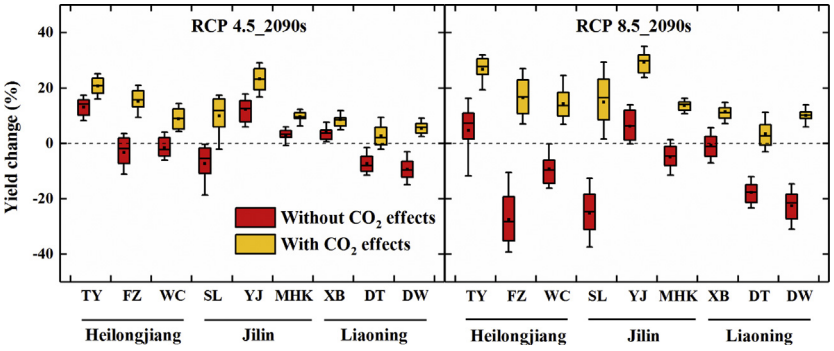

ARTICLE INFO

Article history:
Received 30 November 2018
Received in revised form 26 January 2019
Accepted 31 January 2019
Available online 31 January 2019

Editor: Jay Gan

Keywords:
Future climate change
Impact
Rice
Yield
Northeast China

ABSTRACT

Multi-model ensemble climate projections in combination with crop models are increasingly used to assess the impact of future climate change on agricultural systems. In this study, we used a biophysical process-oriented CERES-Rice crop model driven by downscaled future climate data from 28 Global Climate Models (GCMs) under two emissions scenarios: representative concentration pathway (RCP) 4.5 and RCP8.5, for phase five of the Coupled Model Intercomparison Project (CMIP5) to project the effects of climate change on rice yields in three future time periods in the Northeast China Plain (NECP). The results showed that without consideration of CO_2 effects, rice yield would increase by 1.3%, 1.3%, and 0.4% in the 2030s, 2060s, and 2090s, respectively, under the RCP4.5 scenario. Rice yield would change by +1.1%, −2.3%, and −10.7% in the 2030s, 2060s, and 2090s, respectively, under the RCP8.5 scenario. With consideration of CO_2 effects, rice yield during the 2030s, 2060s, and 2090s would increase by 5.4%, 10.0%, and 11.6% under RCP4.5, and by 6.4%, 12.9%, and 15.6% under RCP8.5, respectively. The rice-growing season would be shortened by 2 to 5 weeks in the future. Overall, the future climate would have positive effects on rice yields in the NECP. Although uncertainties in our study on the impact of climate change on rice might arise from the choice of crop model and GCMs, the results are important for informing policy makers and developing appropriate strategies to improve rice productivity in China.

© 2019 Elsevier B.V. All rights reserved.

* Corresponding author.
E-mail address: zhougs@cma.gov.cn (G. Zhou).

https://doi.org/10.1016/j.scitotenv.2019.01.415
0048-9697/© 2019 Elsevier B.V. All rights reserved.

1. Introduction

Global climate change, which affects natural systems and human society, is a central issue of sustained concern (Xu et al., 2013; IPCC, 2014; Ruane et al., 2014). The agricultural system is one of the most sensitive and vulnerable systems in terms of global climate change (Asseng et al., 2015; He and Zhou, 2016; Lesk et al., 2016). Over the past few decades, climate change has severely affected many agricultural regions and will cause more issues related to food security (Lobell and Gourdji, 2012; IPCC, 2014; Asseng et al., 2015; FAO, 2016). Thus, assessing the impacts of future climate change and ensuring future food security under changing climate conditions is one of the most important themes for the 21st century (Laux et al., 2010; Tilman et al., 2011; Chen et al., 2014; Cui et al., 2018).

China is the world's largest rice producer, and its annual rice production is close to 30% of total worldwide production (FAO, 2018). The Northeast China Plain (NECP) is the largest plain and a significant base of rice production in China. Previous studies have shown a significant impact of climate change on rice production in northeast China; for example, increased temperatures have been beneficial to single rice production in northeast China in the past few decades (Tao et al., 2013; Chen et al., 2017). The rice-growing area has also increased, with the northern limits of the rice cropping system shifting northward because of climate warming (Piao et al., 2010; Liu et al., 2013; Liu et al., 2014; Yang et al., 2015). It is challenging to project future climate change because of the complex nature of climate systems and the uncertainties of crop responses to climate change, which leads to further uncertainty in these studies (IPCC, 2001; Lobell et al., 2006; He et al., 2018). Therefore, it is necessary to establish the range of uncertainty of climate projection and the uncertainty of future climate change effects on rice production to adopt climate change adaptations and ensure the rice supply.

Combining outputs of global climate models (GCMs) or regional climate models (RCMs) under different emission scenarios with process-based crop models is an effective method to investigate the impacts of future climate change on crop production (Xiong et al., 2007; Rosenzweig et al., 2014; Wang et al., 2014). At present, most of the process-based crop models around the world function at the local level (Xiong et al., 2008), one advantage of which is the capacity to deal with interactions among multiple climate factors. Such models can also reveal and quantify the impacts of climate, soil, and management on crop growth and development (Xiao and Tao, 2014; Asseng et al., 2015; Bai and Tao, 2017). However, projections of future climate change are often made on large geographical and time scales (months), whether from GCMs or RCMs, and they are not available to directly drive the crop models at the local level and on a daily time scale. The method that scales historical meteorological data with projected climate data does not consider the changes in climate variability from year to year (Prudhomme et al., 2002). Dynamical downscaling to nest RCMs within GCMs output fields is costly. Thus, we used the statistical downscaling method proposed by Liu and Zuo (2012) to generate realistic future daily climate data at the local level from outputs of raw GCMs; these data were capable of matching crop models to assess the impact of future climate change on agricultural systems.

In this study, we used a well-validated crop model, the CERES-Rice model, driven by future statistically downscaled daily climate data from 28 GCMs for phase five of the Coupled Model Intercomparison Project (CMIP5) under two representative concentration pathway (RCP) scenarios, RCP4.5 and RCP8.5, to project impacts of future climate change on rice yield in the NECP. The objectives of this study were to (1) evaluate the performance of the CERES-Rice model using field trial data in NECP, (2) investigate the impacts of future climate on rice phenology and yield in this region, and (3) identify the relationships among rice yields and climatic variables (solar radiation, mean temperature, precipitation, and CO_2).

2. Materials and methods

2.1. Study sites

The NECP, which includes Heilongjiang, Jilin, and Liaoning Provinces, is the largest plain in China. The soil in the plain mainly contains Phaeozem and Chernozem, and it is one of the most fertile soil regions in the world (Xu et al., 2010). The NECP encompasses temperate and warm temperate zones, characteristic of the continental monsoonal climate. Annual rainfall ranges between 400 and 1100 mm, and annual temperature ranges from −5 to 11 °C. The main rice planting system is single rice cultivation. Because of the excellent geographical environment and favorable natural resources, the NECP region is quite suitable for single rice growing from May to September.

In this study, we selected nine representative agro-meteorological stations across a north-to-south transect of the NECP to simulate single rice yield (Fig. 1). These observed field stations were distributed evenly in the main rice areas of Heilongjiang, Jilin, and Liaoning Provinces and covered different climatic and geographic conditions. Field trial data (e.g., cultivar, phenological dates, agronomic management, and yield components) at each station were recorded, as well as the corresponding meteorological and soil conditions. Detailed information about each station is shown in Table 1.

2.2. Experimental and climate data

The field trial data at nine stations during 2006–2010 were obtained from the Chinese Meteorological Administration (CMA). Records included rice variety name, phenology (transplanting, heading, and maturity dates), yield and yield components (grain number per spike, 1000-grain weight, and harvest index), and agronomic management (planting density and nitrogen application rate), which were used to calibrate and validate the CERES-Rice model. Soil profile data of all the stations were obtained from the 1:1 Million scale Soil Map of China included in the Harmonized World Soil Database (HWSD) version 1.2 (Shi et al., 2004; FAO/IIASA/ISRIC/ISS-CAS/JRC, 2012). The soil database included soil texture, bulk density, pH, organic matter content, and cation exchange capacity, which were required to run the model. Data of total nitrogen content were obtained from the China Soil Database (CSSD): http://vdb3.soil.csdb.cn/.

Observed daily meteorological data of all stations during 1960 to 2010 were obtained from the Chinese Meteorological Data Service Center (CMDC): http://data.cma.cn/en. Daily solar radiation ($MJ \cdot m^{-2}$), daily maximum and minimum temperatures (°C), and daily precipitation (mm) were summarized. For future climate, outputs of 28 GCMs were selected from CMIP5 (Table 2), under two RCP scenarios (RCP4.5 and RCP8.5) in three time periods of the 21st century: the 2030s (2021–2040), the 2060s (2051–2070), and the 2090s (2081–2100). We planned to use as many climate models as possible to establish the range of uncertainty of climate projection, and then span the uncertainty of climate change impact on rice yield. The monthly data simulated by the GCMs were statistically downscaled to the specific stations. This process corrected biases in the site-based monthly GCMs values; then, daily climate variables were temporally scaled through the WGEN stochastic weather generator based on the spatially downscaled monthly data. The complete method was developed and described by Liu and Zuo (2012) and widely used to project the impacts of future climate change on agricultural systems in recent years (Yang et al., 2014; Anwar et al., 2015; Guo et al., 2016; Wang et al., 2016; Liu et al., 2017; He et al., 2018; Wang et al., 2018). Unlike other downscaling methods that use complicated data, this method used historical observed climate data to modify the monthly GCMs data and was capable of rapid downscaling from outputs of raw GCMs.

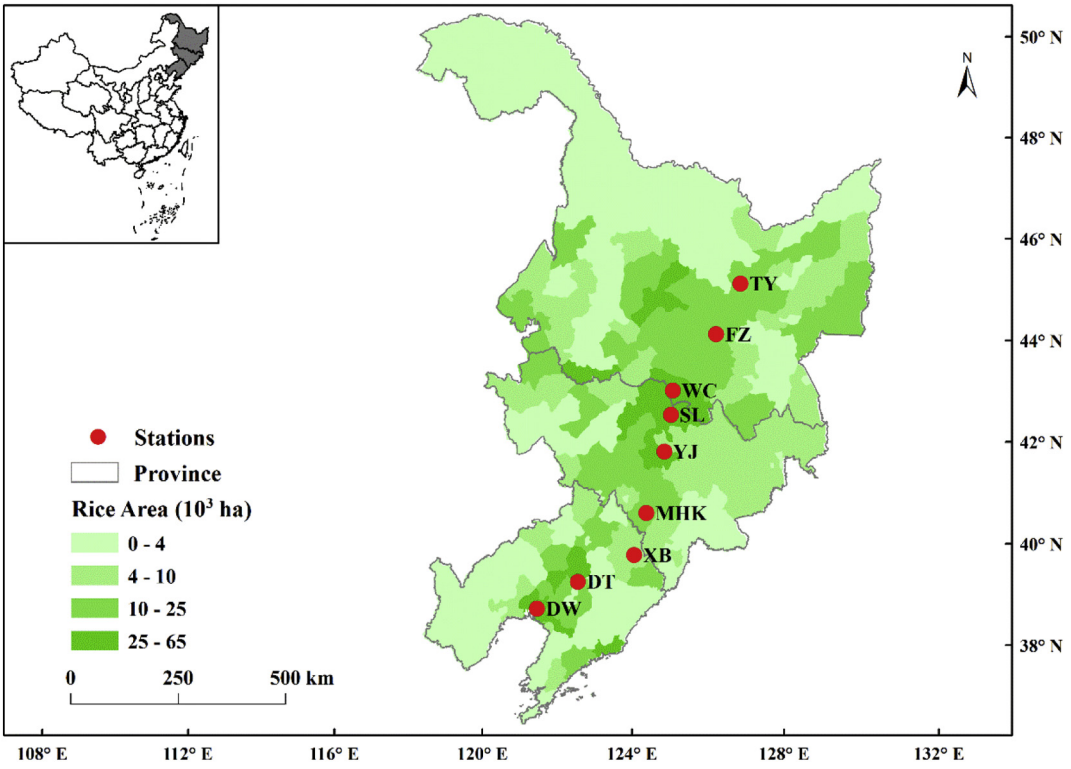

Fig. 1. Location of nine stations selected in the Heilongjiang, Jilin, and Liaoning Provinces of the Northeast China Plain.

2.3. CERES-Rice model

The CERES-Rice model used in this study was included in Decision Support System for Agro-technology Transfer (DSSAT) version 4.7 (Jones et al., 2003; Hoogenboom et al., 2017). The CERES-Rice model is a biophysical process-oriented crop model driven by daily climate data (solar radiation, maximum and minimum temperatures, and precipitation). It can simulate rice growth, development, photosynthesis,

Table 1
Detailed information at all nine representative stations in the Northeast China Plain.

Stations	Tangyuan (TY)	Fangzheng (FZ)	Wuchang (WC)	Shulan (SL)	Yongji (YJ)	Meihekou (MHK)	Xinbin (XB)	Dengta (DT)	Dawa (DW)
Geolocation									
Provinces	Heilongjiang	Heilongjiang	Heilongjiang	Jilin	Jilin	Jilin	Liaoning	Liaoning	Liaoning
Latitude (°N)	46.7	45.8	44.9	44.4	43.7	42.5	41.7	41.4	41.0
Longitude (°E)	129.9	128.8	127.2	126.9	126.5	125.6	125.1	123.3	122.1
Altitude (m)	95.1	119.3	194.6	250.6	229.5	340.5	328.4	36.8	5.5
Climate (May to September)									
SRD (MJ m^{-2})	16.9	16.6	17.2	16.9	16.4	16.8	16.7	17.1	18.5
T_{max} (°C)	24.0	23.8	24.0	24.7	24.0	24.6	26.0	26.5	25.8
T_{min} (°C)	13.0	12.3	12.2	13.7	12.7	13.9	13.7	16.2	17.9
Precipitation (mm)	439.3	480.8	535.7	430.2	567.4	557.4	617.6	553.3	512.1
Crop									
Calibration data	2006–2007	2006	2007	2008	2007	2007	2006	2006	2006
Validation data	2008, 2010	2007–2008	2008–2009	2009	2008	2008	2007	2007–2008	2007
Cultivar	XX1	KD10	WYD4	PJ7	JJ88	FY307	TF8	LJ294	YF47
Transplanting date (m/d)	5/20	5/21	5/15	5/20	5/24	5/30	5/31	5/22	5/23
Maturity date (m/d)	9/24	9/11	9/15	9/20	9/18	9/22	9/27	9/24	9/27
Soil									
Soil texture	Loam	Loam	Loam	Loam	Loam	Loam	Loam	Loam	Clay
Organic carbon (%)	0.7	2.0	0.8	2.0	0.8	0.8	0.8	2.0	0.5
Total N (%)	0.2	0.2	0.2	0.1	0.1	0.1	0.1	0.1	0.1
Management									
Irrigation	Irrigation	Irrigation	Irrigation	Irrigation	Irrigation	Irrigation	Irrigation	Irrigation	Irrigation
Fertilizer	Chemical fertilizer	Chemical fertilizer	Chemical fertilizer	Chemical fertilizer	Chemical fertilizer	Chemical fertilizer	Chemical fertilizer	Chemical fertilizer	Chemical fertilizer

SRD: solar radiation; T_{max}: maximum temperature; T_{min}: minimum temperature; m/d: month/date.

Table 2
Information on the 28 global climate models (GCMs) selected in this study for statistically downscaled outputs of nine stations in the Northeast China Plain.

ID	GCM	Code	Country
1	BCC-CSM 1.1	BC1	China
2	BCC-CSM 1.1 (m)	BC2	China
3	BNU-ESM	BNU	China
4	CanESM2	CaE	Canada
5	CCSM4	CCS	USA
6	CESM1(BGC)	CE1	USA
7	CMCC-CM	CM2	Europe
8	CMCC-CMS	CM3	Europe
9	CSIRO-Mk3.6.0	CSI	Australia
10	EC-EARTH	ECE	Europe
11	FIO-ESM	FIO	China
12	GISS-E2-H-CC	GE2	USA
13	GISS-E2-R	GE3	USA
14	GFDL-CM3	GF2	USA
15	GFDL-ESM2G	GF3	USA
16	GFDL-ESM2M	GF4	USA
17	HadGEM2-AO	Ha5	Korea
18	INM-CM4	INC	Russia
19	IPSL-CM5A-MR	IP2	France
20	IPSL-CM5B-LR	IP3	France
21	MIROC5	MI2	Japan
22	MIROC-ESM	MI3	Japan
23	MIROC-ESM-CHEM	MI4	Japan
24	MPI-ESM-LR	MP1	Germany
25	MPI-ESM-MR	MP2	Germany
26	MRI-CGCM3	MR3	Japan
27	NorESM1-M	NE1	Norway
28	NorESM1-ME	NE2	Norway

respiration, and dry matter distribution. It also simulates soil water balance and nitrogen balance and accounts for the effects of CO_2 concentration in the process of rice growth. The minimum input data sources required are weather, soil, and cultivar-specific genetic parameters. Detailed descriptions of the CERES-Rice model can be found at the website: http://dssat.net/. The CERES-Rice model has been widely applied in many countries, including China (Yun, 2003; Tao et al., 2008a; Kim et al., 2013), and one of its advantages is that in DSSAT, it provides the ability to ingest year-varying values of atmospheric CO_2 concentration, which make it suitable for assessing the effects of future CO_2 concentration on rice production.

2.4. Simulation and analysis

We calibrated and validated the CERES-Rice model at all stations using observed field data from 2006 to 2010. Based on the field trial records, the rice variety most frequently planted during 2006–2010 at each station was regarded as the typical local variety (Table 1). Similarly, the typical agronomic management practices (e.g., transplanting date, planting density, and nitrogen application rate) at each station were summarized from field records during 2006–2010. The actual records for management were used for model calibration, validation, and future simulation at each site. Rice at all stations was irrigated, which had sufficient water supply; therefore, the irrigations were set to automatic (i.e., when moisture content was <50% of water capacity at 30 cm depth, the rice was irrigated with 10 mm of water). The field trial data of the first 1 to 2 years were used to calibrate the CERES-Rice model, and data from the other years were used for validation.

We used the validated CERES-Rice model to simulate rice phenology and yield under baseline (1991–2010) and future climate conditions with and without CO_2 effects. The average CO_2 concentration ($[CO_2]$) of 380 ppm was set when simulating baseline yield and yield under future climate scenarios without consideration for CO_2 effects. With consideration for CO_2 effects, future $[CO_2]$ for RCP4.5 and RCP8.5 was calculated by empirical functions of calendar year (Liu et al., 2017; Wang et al., 2017; Wang et al., 2018). Under RCP4.5 and RCP8.5, the $[CO_2]$ of each year during 2021–2100 was calculated, respectively, as follows:

$$[CO_2] = 650.18 + \frac{7.5326 \times 10^{-5} y - 0.16276}{2.2299 \times 10^{-4} - 727.97 y^{-2}} - 1.8747 \times 10^{-4}(y-2045)^3 \quad (1)$$

$$[CO_2] = 1034.3 + \frac{267.78 - 1.6188 y}{4.0143 + 53.342 y^{-5.2822}} + 2.1746 \times 10^{-5}(y-2020)^3 + 1.0065 \times 10^{-4}(y-1911)^3 \quad (2)$$

where y was the calendar year from 2021 to 2100 (i.e., $y = 2021, 2022, \ldots, 2100$). Then, the ensemble average of all the yield results in each period under different scenarios was calculated and compared with the baseline yield.

A stepwise regression model was used to estimate the impact of various climate factors (solar radiation, mean temperature, precipitation, and $[CO_2]$) on future rice yield:

$$\Delta Y = a\Delta S + b\Delta Tmn + c\Delta P + d\Delta CO_2 \quad (3)$$

where ΔS, ΔTmn, ΔP, and ΔCO_2 were the changes in solar radiation, mean temperature, precipitation, and $[CO_2]$ during the rice-growing period (1 May to 30 September) for the 2030s, 2060s, and 2090s compared with the 1991–2010 baseline under RCP4.5 and RCP8.5 of all 28 GCMs at each station. ΔY represented the corresponding yield changes, and a, b, c, and d were model parameters.

2.5. Model performance assessment

To compare model performance, we computed the following validation indices: (1) the normalized root mean squared error (RMSE%), and (2) the index of agreement (D_{index}) (Willmott, 1982):

$$RMSE(\%) = \frac{100}{\bar{O}}\sqrt{\frac{1}{n}\sum_{i=1}^{n}(P_i - O_i)^2} \quad (4)$$

$$D_{index} = 1 - \frac{\sum_{i=1}^{n}(P_i - O_i)^2}{\sum_{i=1}^{n}\left(|P_i - \bar{O}| + |O_i - \bar{O}|\right)^2} \quad (5)$$

where P_i was the simulated value in the ith year, O_i was the observed value in the ith year, and $\bar{O}$ was the average of the observed values of the n years.

3. Results

3.1. Calibration and validation of the CERES-Rice model

The validated results showed that the simulated dates of heading and maturity were consistent with observed dates (Fig. 2a, b). The errors of simulated heading and maturity dates were within 5% of the observed mean, and the D_{index} values were 0.98 and 0.88, respectively. The simulated yields were also in good general agreement with observed values (Fig. 2c). Compared with those of observed yields, the relative errors of simulated yields were <10%, and the D_{index} was close to 1.0. The validated CERES-Rice model efficiently reproduced the measured phenology and could explain 89% of the variation in rice yield. Consequently, it was suitable for simulating the dynamics of phenology and yield for rice in the NECP.

3.2. Projected climate change during rice growth period in the future

Under the RCP4.5 scenario, the ensemble-mean solar radiation increased from 0.0 to 0.1 $MJ \cdot m^{-2}$, 0.4 to 0.5 $MJ \cdot m^{-2}$, and 0.4 to

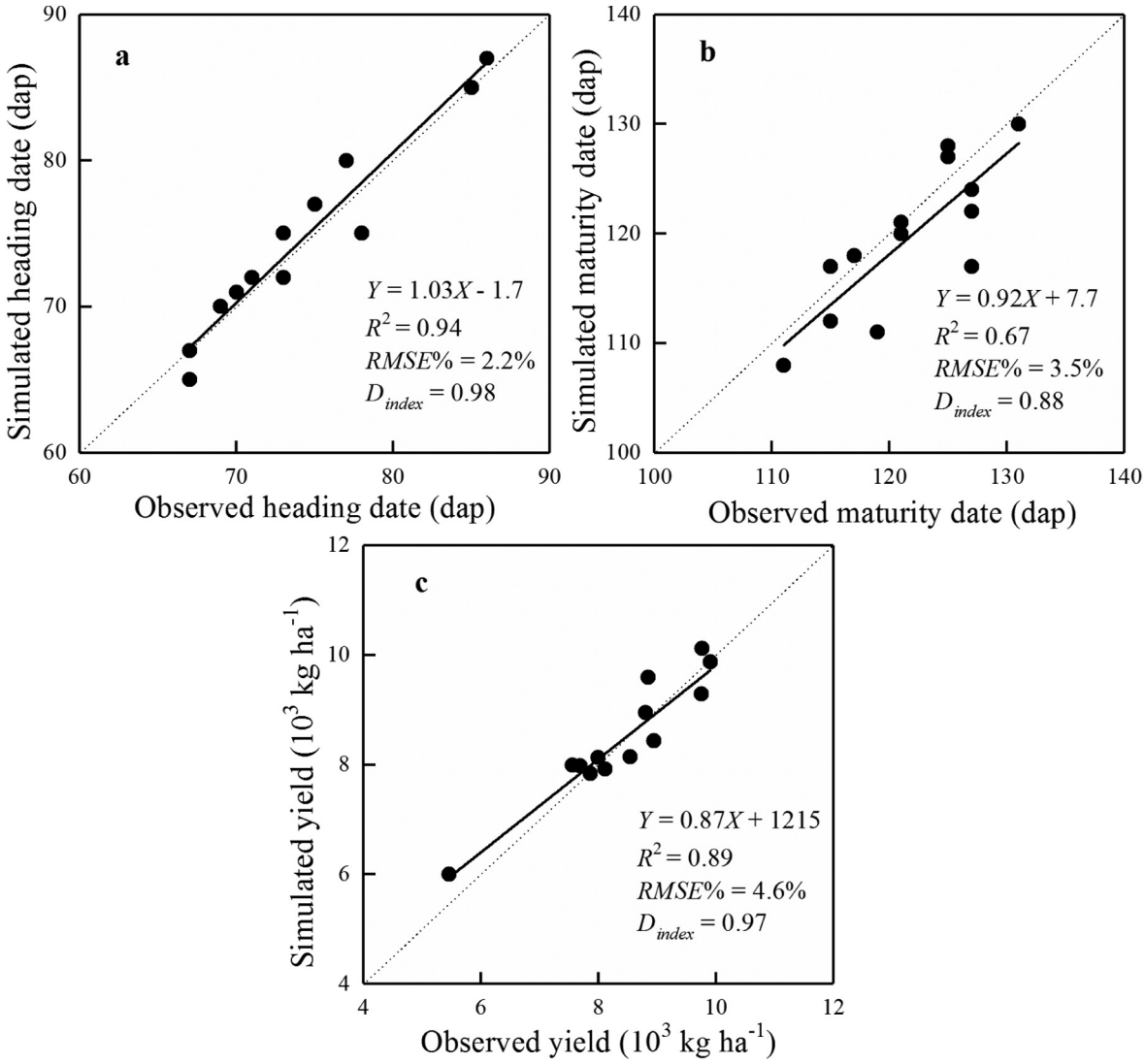

Fig. 2. Simulated and observed phenology and yield at all stations. dap: days after transplanting.

0.7 MJ·m^{-2} across the nine stations in the NECP during the 2030s, 2060s, and 2090s, respectively, and from 0.0 to 0.1 MJ·m^{-2}, 0.3 to 0.6 MJ·m^{-2}, and 0.5 to 0.8 MJ·m^{-2} during the 2030s, 2060s, and 2090s under RCP8.5, respectively (Fig. 3). In the 2030s, solar radiation showed little change under RCP4.5 and RCP8.5. In the 2060s, solar radiation increased, but there was not much difference between RCP4.5 and RCP8.5. In the 2090s, solar radiation increased continuously and solar radiation under RCP8.5 increased slightly more than that under RCP4.5. In general, solar radiation showed an increasing trend during the future rice growth period, especially in the 2060s and 2090s.

Under RCP4.5, the ensemble-mean maximum temperature (T_{max}) increased from 0.5 to 0.8 °C, 1.1 to 1.6 °C, and 1.4 to 1.8 °C during the 2030s, 2060s, and 2090s in the NECP (Fig. 4). The ensemble-mean minimum temperature (T_{min}) increased from 0.8 to 1.0 °C, 1.5 to 1.7 °C, and 1.8 to 2.1 °C during the 2030s, 2060s, and 2090s respectively (Fig. 4).

Under RCP8.5, the ensemble-mean T_{max} changed from 0.6 to 1.0 °C, 1.7 to 2.4 °C, and 2.9 to 4.1 °C during the 2030s, 2060s, and 2090s in the NECP, respectively (Fig. 5). The ensemble-mean T_{min} changed from 0.9 to 1.1 °C, 2.4 to 2.7 °C, and 3.8 to 4.7 °C during the 2030s, 2060s, and 2090s, respectively (Fig. 5). In the 2030s, differences in temperature increases were not obvious between RCP4.5 and RCP8.5. In the 2060s, the increased temperature under RCP8.5 was higher than that under RCP4.5 by about 0.8 °C. In the 2090s, the temperature increase under RCP8.5 was higher than that under RCP4.5 by about 2.2 °C. In future periods, T_{min} increased more than T_{max}. The results showed that projections of T_{max} and T_{min} from 28 GCMs had wide ranges, and the ranges became wider over time. However, most of the outputs from the GCMs and the ensemble-mean changes in temperature were increased overall.

3.3. Projected changes in rice phenology in the future

Climate change could lead directly to changes in crop phenology, further affecting crop yield. Our results showed that the rice growth period would be shorter in the future at all stations (Figs. 6, 7), particularly after 2050. Under RCP4.5, the average length of the vegetative growth period was shortened by 2.5 to 4.9 days, 5.0 to 8.1 days, and 6.2 to 9.8 days during the 2030s, 2060s, and 2090s in the NECP, respectively (Fig. 6). Under RCP8.5, the average length of the vegetative growth period was shortened by 2.8 to 5.6 days, 7.4 to 11.6 days, and 11.2 to 19.2 days during the 2030s, 2060s, and 2090s, respectively (Fig. 6). Changes in length of the vegetative growth period had a wider range over time, and changes were greater in stations at a higher latitude that in those at a lower latitude. For example, the vegetative growth period changed from −12.1 days (10th percentile, Q10) to −2.9 days

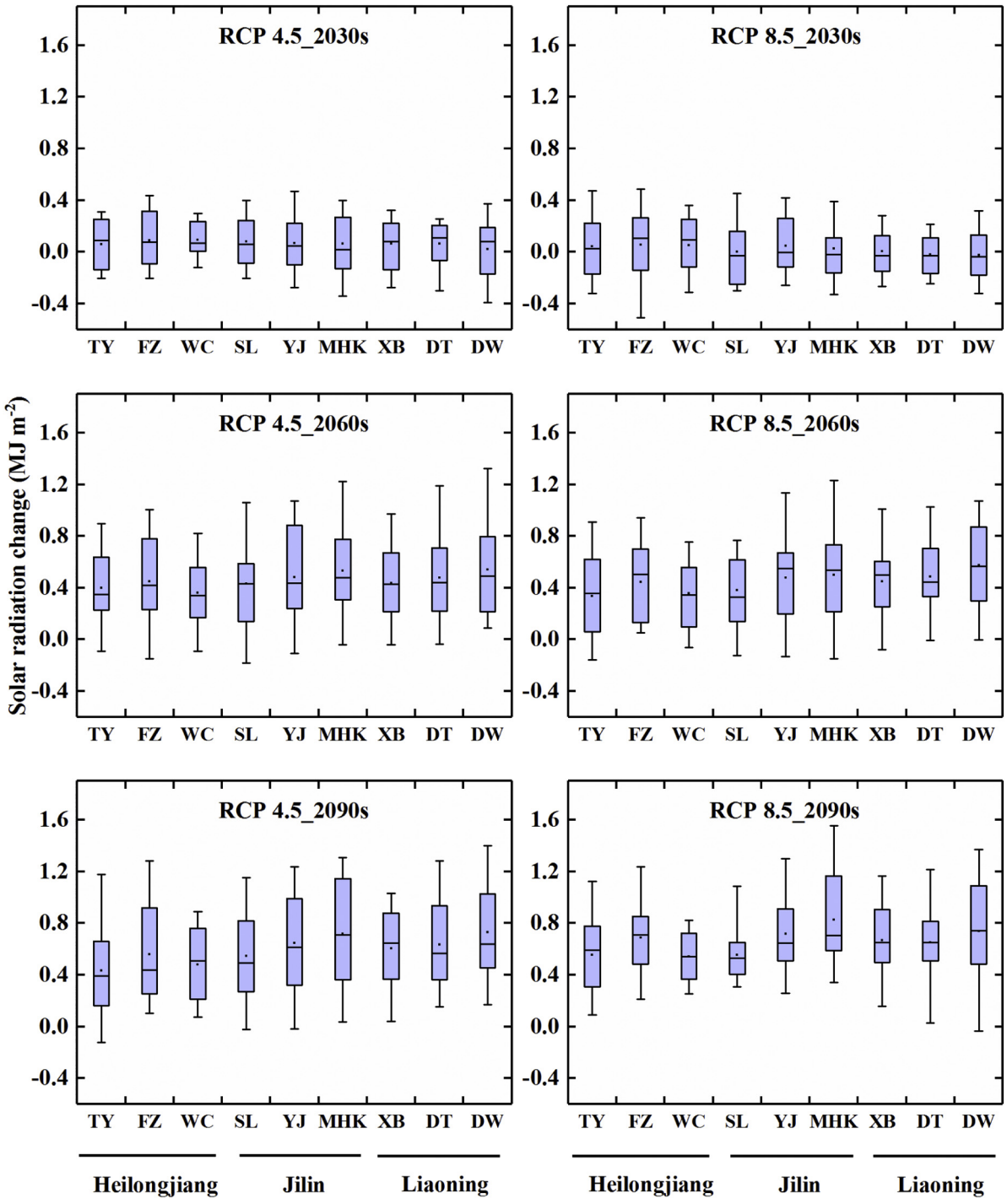

Fig. 3. Projected change in solar radiation during the rice-growing period (May to September) for the 2030s, 2060s, and 2090s compared with 1991–2010 under the representative concentration pathway (RCP)4.5 and RCP8.5 scenarios using 28 global climate models (GCMs) for nine stations in the Northeast China Plain. The x-axis indicates the nine stations from higher to lower latitude in each province. The box boundaries indicate the 25th and 75th percentiles; the black line and dot within the box mark the median and mean, respectively; and whiskers below and above the box indicate the 10th and 90th percentiles, respectively.

(90th percentile, Q90) in the 2060s, and from −15.1 days (Q10) to −3.0 days (Q90) in the 2090s at the TY station (highest latitude) in RCP4.5 (Fig. 6). The vegetative growth period changed from −7.9 days (Q10) to −2.0 days (Q90) in the 2060s, and from −9.1 days (Q10) to −3.2 days (Q90) in the 2090s at the DW station (lowest latitude) in RCP4.5 (Fig. 6).

For the reproductive growth period, under RCP4.5, the average length of the reproductive growth period was shortened by 5.5 to 13.7 days, 8.6 to 21.6 days, and 9.5 to 23.3 days during the 2030s, 2060s, and 2090s, respectively (Fig. 7). Under RCP8.5, the average length of the reproductive growth period was shortened by 6.5 to 15.2 days, 11.5 to 28.1 days, and 14.1 to 34.3 days during the 2030s, 2060s, and 2090s, respectively (Fig. 7). There were large variations of the reproductive growth period changes in the 2060s and 2090s. For example, the reproductive growth period changed from −30.2 days (Q10) to −11.8 days (Q90) in the 2060s, and from −31.4 days (Q10) to −12.5 days (Q90) in the 2090s at the TY station in RCP4.5 (Fig. 7).

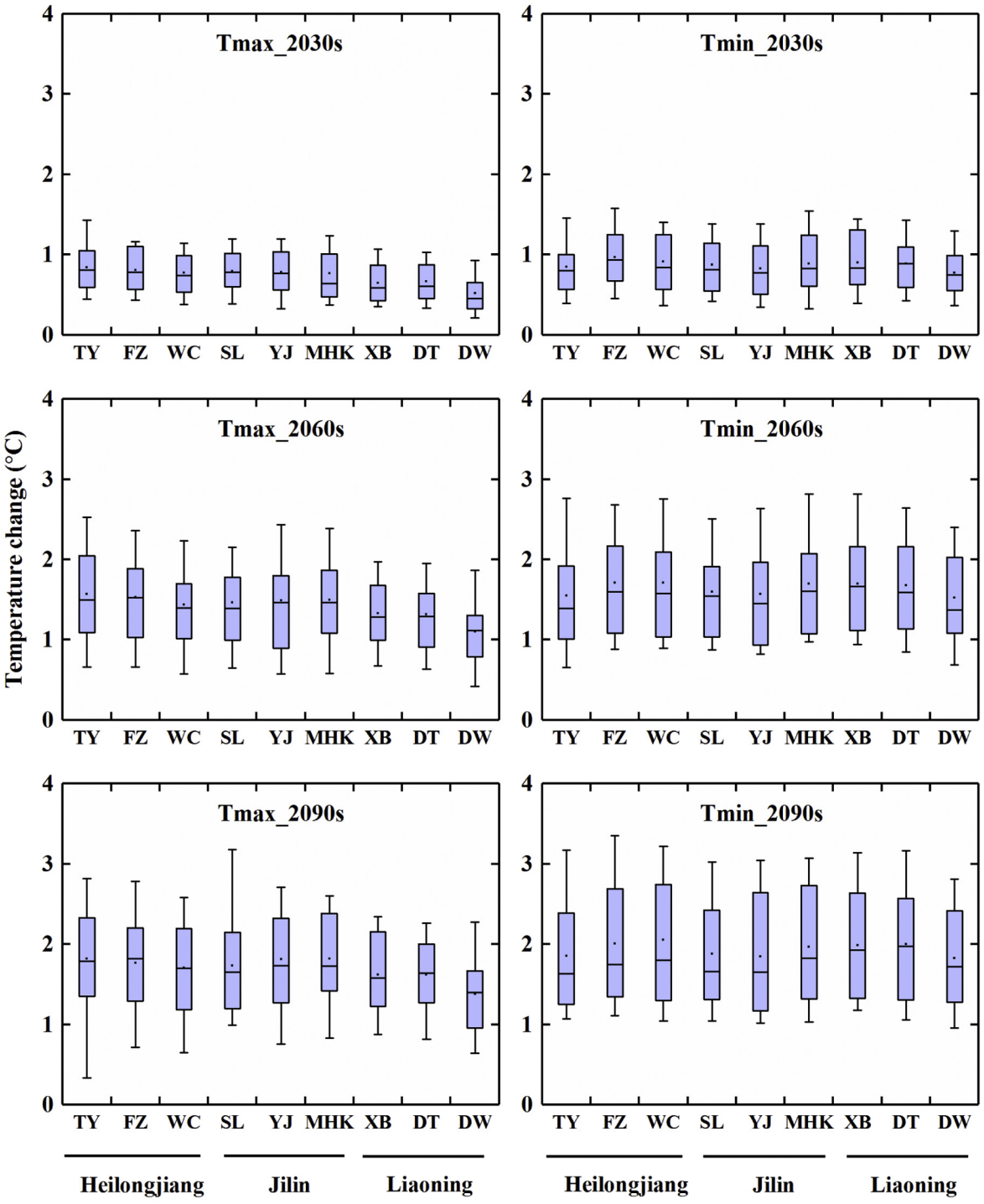

Fig. 4. Projected change in maximum and minimum temperatures (T_{max} and T_{min}) during the rice-growing period (May to September) for the 2030s, 2060s, and 2090s compared with 1991–2010 under the representative concentration pathway (RCP)4.5 scenario using 28 global climate models (GCMs) for nine stations in the Northeast China Plain. The x-axis indicates the nine stations from higher to lower latitude in each province. The box boundaries indicate the 25th and 75th percentiles; the black line and dot within the box mark the median and mean, respectively; and whiskers below and above the box indicate the 10th and 90th percentiles, respectively.

All outputs from GCMs showed that the vegetative growth period of rice in NECP would shorten in the future. The reproductive growth period showed the same characteristic changes as the vegetative growth period.

3.4. Projection of future rice yield changes with and without CO_2 effect

When CO_2 effects were not considered, rice yield changed from −4.3% to 10.7% in the 2030s, from −6.9% to 13.7% in the 2060s, and from −9.4% to 13.1% in the 2090s under RCP4.5 (Fig. 8). Across all stations, rice yield increased the most in TY, in the north of Heilongjiang Province, and decreased the most in DW, in the south of Liaoning Province. In the 2030s under RCP8.5, rice yield changed in a manner similar to that under the RCP4.5 scenario. Rice yield changed from −6.0% to 11.4% compared with the 1991–2010 baseline. In the 2060s, yield decreased slightly by, on average, 2.3%, from −12.4% to 12.7%. In the 2090s, yield decreased notably at most stations of NECP, ranging from −0.7% to −27.5%, and increased in a few stations, ranging from 4.7%

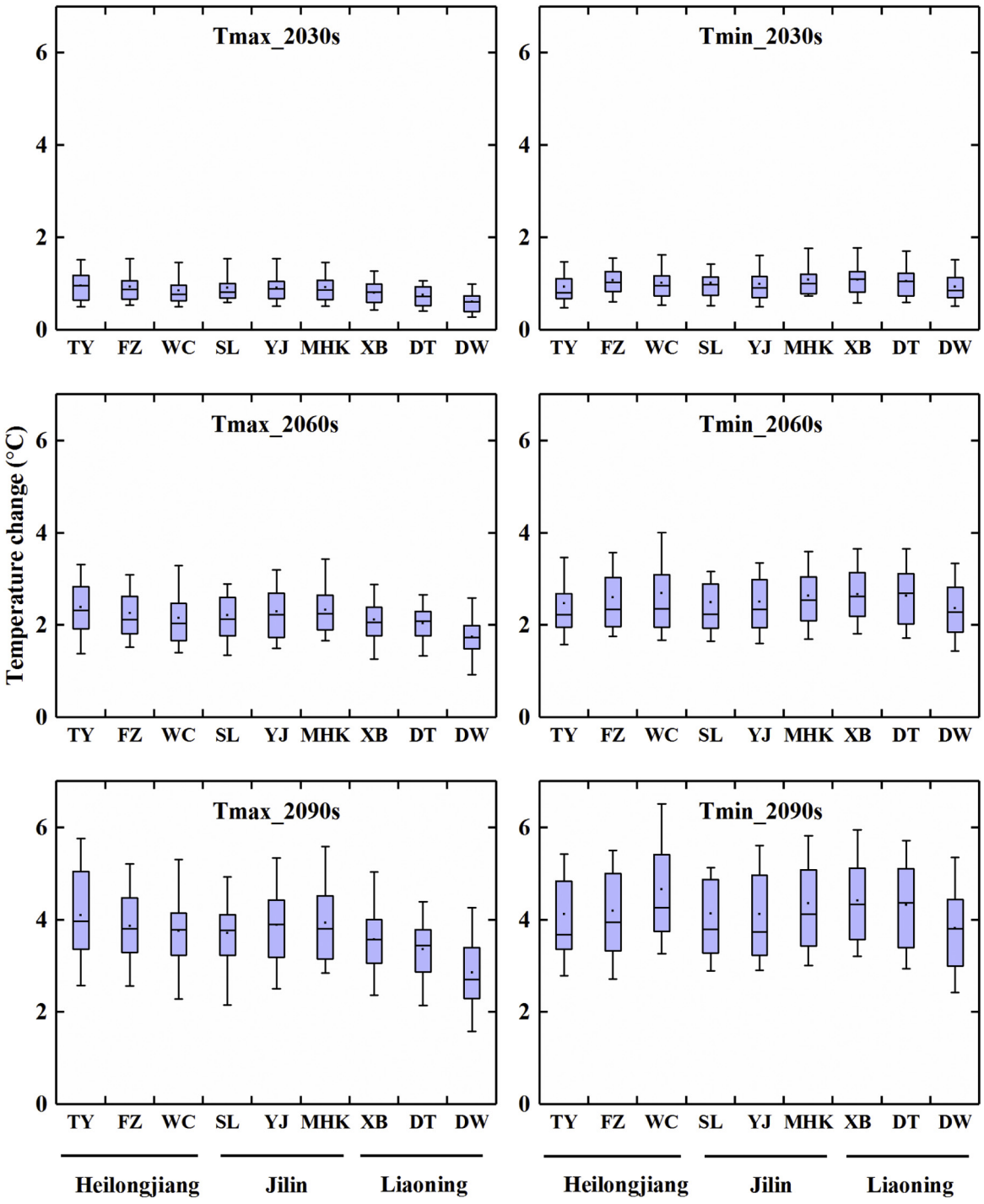

Fig. 5. Projected change in maximum and minimum temperatures (T_{max} and T_{min}) during the rice-growing period (May to September) for the 2030s, 2060s, and 2090s compared with 1991–2010 under the representative concentration pathway (RCP)8.5 scenario using 28 global climate models (GCMs) for nine stations in the Northeast China Plain. The x-axis indicates the nine stations from higher to lower latitude in each province. The box boundaries indicate the 25th and 75th percentiles; the black line and dot within the box mark the median and mean, respectively; and whiskers below and above the box indicate the 10th and 90th percentiles, respectively.

to 6.2%. The TY station in Heilongjiang Province was the station where rice yield increased the most in the 2030s and 2060s under RCP8.5, and the DW station, in the south of Liaoning Province, showed the greatest reduction in yield in the 2030s and 2060s.

Yields benefit from increased [CO_2] in the future under both RCP4.5 and RCP8.5 (Fig. 8). When CO_2 effects are considered, yield would change from 0.2% to 13.3% in the 2030s, from 2.5% to 20.2% in the 2060s, and from 2.7% to 23.4% in the 2090s under RCP4.5. Under RCP8.5, yield would change from 0.9% to 15.6% in the 2030s, from 3.2% to 25.5% in the 2060s, and from 3.5% to 29.4% in the 2090s. There was little difference between yields under RCP4.5 and RCP8.5 in the 2030s. In the 2060s, effects of CO_2 on rice yields were significantly greater than that in the earlier decades, especially under RCP8.5. In the 2090s, CO_2 played a larger role in increasing yield and shifted the trend from a yield reduction to an increase in RCP8.5.

We observed large variations in yield changes in the 2060s and 2090s, especially under RCP8.5. For example, yield changed from

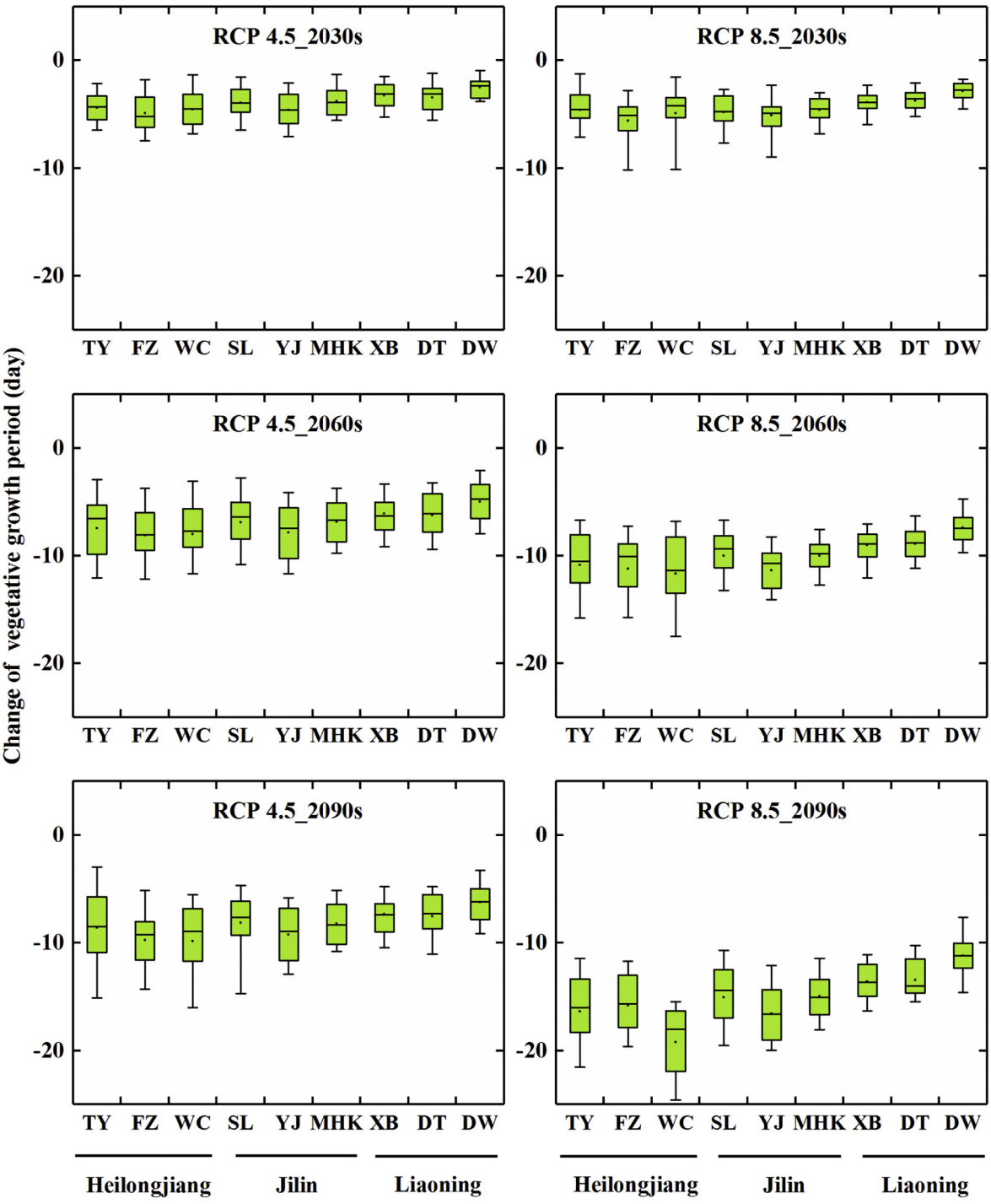

Fig. 6. Simulated change in the vegetative growth period in the 2030s, 2060s, and 2090s under representative concentration pathway (RCP)4.5 and RCP8.5 scenarios relative to 1991–2010 using 28 global climate models (GCMs) for nine stations in the Northeast China Plain. The box boundaries indicate the 25th and 75th percentiles; the black line and dot within the box mark the median and mean, respectively; and whiskers below and above the box indicate the 10th and 90th percentiles, respectively.

−39.2% (Q10) to −10.5% (Q90) without consideration for CO_2 effects, and from 7.1% (Q10) to 27.0% (Q90) with consideration for CO_2 effects in the 2090s at the FZ station under RCP8.5.

3.5. Rice yield relationship with future climate

The stepwise regression analysis showed that yield change was strongly correlated with changes in [CO_2], solar radiation, and mean temperature but was not significantly correlated with precipitation in the future (Table 3). Increases in solar radiation and [CO_2] during the rice growth period would increase rice yields significantly in the NECP. We detected a significant negative correlation between yield change and mean temperature in Jilin and Liaoning Provinces (Table 3). Yields in Jilin and Liaoning Provinces would decrease 2.19% and 1.42%, respectively, with a 1.0 °C increase in mean temperature. Overall, three climate factors—[CO_2], solar radiation, and mean temperature—could explain >60% of the change in future rice yield.

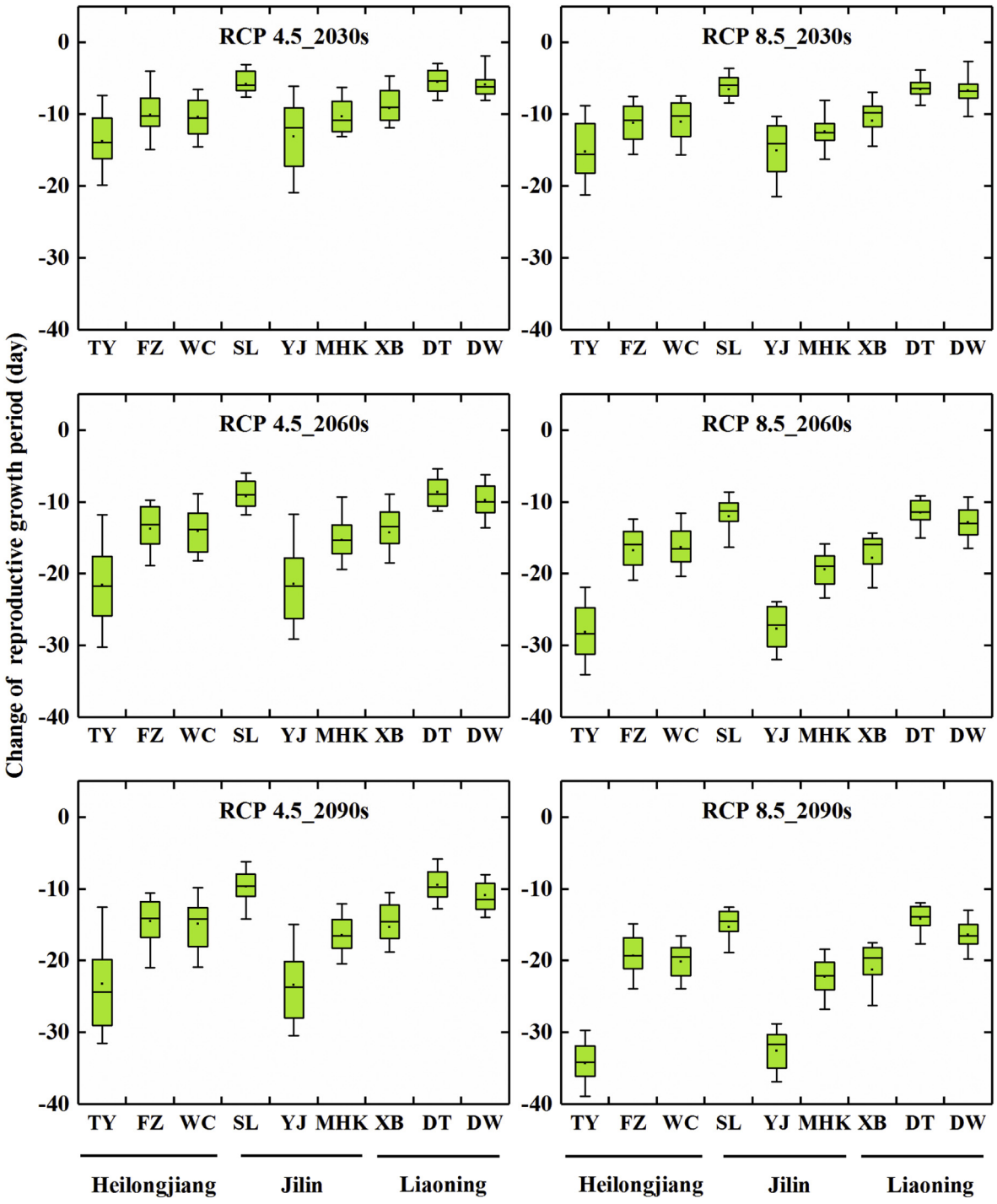

Fig. 7. Simulated change in the reproductive growth period in the 2030s, 2060s, and 2090s under representative concentration pathway (RCP)4.5 and RCP8.5 scenarios relative to 1991–2010 using 28 global climate models (GCMs) for nine stations in the Northeast China Plain. The box boundaries indicate the 25th and 75th percentiles; the black line and dot within the box mark the median and mean, respectively; and whiskers below and above the box indicate the 10th and 90th percentiles, respectively.

4. Discussion

4.1. Model performance

The performance of crop models needs to be validated before applying them to future simulations. We tested the CERES-Rice model at our study sites and found that it simulated rice growth well in the NECP. There was a good agreement between simulated and observed phenology and yield; for example, the R^2 and RMSE% between the simulated and observed yield were 0.89 and 4.6%, respectively. Similar results have been obtained in previous rice studies (Tao et al., 2008a; Kim et al., 2013). For example, Kim et al. (2013) validated the CERES-Rice models in Gwangju, Korea, and the correlation coefficient of simulated and observed yield was 0.91. For other rice models or crop models, simulation results have similar errors in different regions (Xiao and Tao, 2014; Bai et al., 2016). As a result, we believe that the validated CERES-Rice model has an acceptable error rate and could capture the impacts of climate change on rice yield in the NECP.

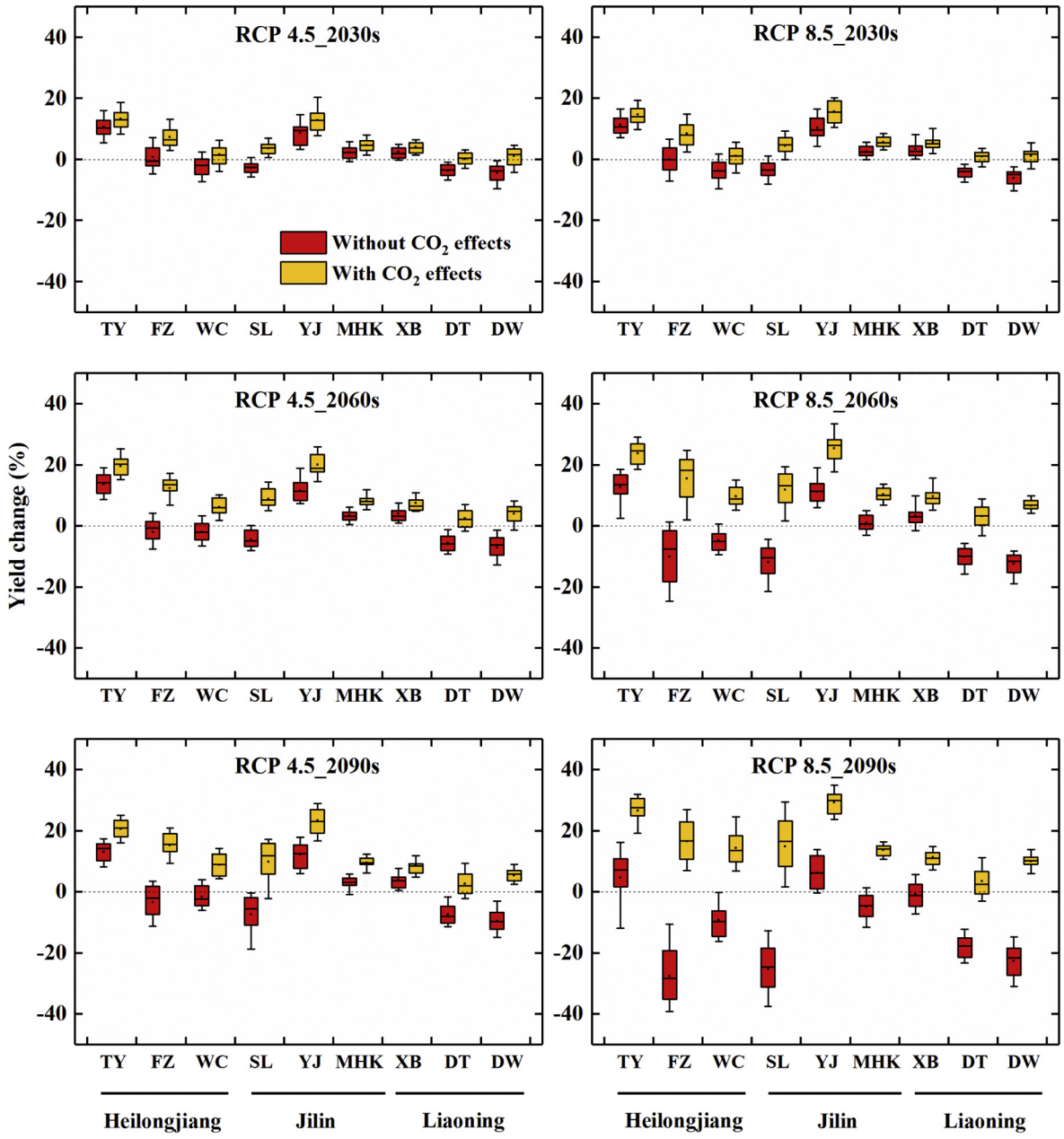

Fig. 8. Simulated rice yield change (compared with baseline 1991–2010) in the 2030s, 2060s, and 2090s under representative concentration pathway (RCP) 4.5 and RCP8.5 scenarios relative to 1991–2010 using 28 global climate models (GCMs) for nine stations in the Northeast China Plain. The box boundaries indicate the 25th and 75th percentiles; the black line and dot within the box mark the median and mean, respectively; and whiskers below and above the box indicate the 10th and 90th percentiles, respectively.

4.2. Yield change under future climate change

Our simulations projected that multi-model mean rice yield increased by 5.4% under RCP4.5 and by 6.4% under RCP8.5 compared with baseline climate across the nine locations by the 2030s with consideration of CO_2 effects. A greater increase was found in the 2060s and 2090s under both RCP scenarios. Our simulated results were consistent with those of Yang et al. (2015), who showed that rice production would increase in China under future projections of increased temperatures and elevated CO_2 concentrations. In our study, the greatest yield increases were found in the northern part of the region, consistent with the yield increases being generally greater at higher latitudes (Kim et al., 2013). This is because the response of yield to temperature changes were, to some extent, related to baseline temperature (Berg et al., 2013). At higher latitudes, where temperatures are lower, a small increase in temperature would likely have a larger effect on yield increase.

Solar radiation is an important source of energy for crop growth, development, biomass accumulation, and geographical distribution. Our results exhibited a positive relationship between solar radiation and rice yield in the NECP, which was consistent with previous findings

Table 3
Coefficients in the stepwise regression analysis on the impacts of future climate change in rice growth period (May to September) on rice yield (%).

Provinces	ΔCO_2 (100 ppm)	ΔS (MJ m^{-2})	ΔTmn (°C)	ΔP (%)	R^2
Heilongjiang	4.90***	3.89***	–	–	0.68
Jilin	6.43***	6.10***	−2.19***	–	0.68
Liaoning	2.84***	3.39***	−1.42***	–	0.60

*** Significant at $p < 0.001$.

(Tao et al., 2013). In our study, future projections showed that solar radiation would increase during the rice growth period, especially in the 2060s and 2090s, which would be beneficial for rice yield in the NECP.

Over the past few decades, climate warming created thermal conditions that promoted a substantial increase in cropland area (Shi et al., 2014). Higher temperatures did not cause high-temperature stress but reduced low-temperature stress in the NECP (Sun and Huang, 2011), and because of an increase in minimum temperature, rice yields were estimated to increase by 4.5% to 14.6% per 1 °C (Tao et al., 2008b). Our results also indicated that climate warming would be positive for rice yield in a certain future in the NECP, especially in the northern part.

Future temperature change would shorten the rice growth period in the NECP. Our simulations projected that the multi-model mean rice growing period would be shorter by 13.2 days under RCP4.5 and by 15.1 days under RCP8.5 compared with the baseline climate across the nine locations by the 2030s. A greater reduction in length can be expected in the 2060s and 2090s under both RCP scenarios; these results are consistent with previous studies (Tao et al., 2008a; Wu et al., 2014). For example, Wu et al. (2014) found that the rice-growing season in the 2020s would shorten by 1.8 to 21.6 days because of climate change. The reduction in length of the whole growth period would result in insufficient rice growth with less dry matter stored in grain, resulting in reduced yields. In the face of increased temperature, adjusting the planting date, developing high thermal requirements, and developing rice cultivars with high heat tolerance might be effective ways of tackling climate change.

4.3. Effects of CO_2 fertilization on rice yield

Carbon dioxide is an important factor in the effect of climate change on agricultural systems (Ruane et al., 2014). CO_2 and temperature affect the rate of light-saturated photosynthesis and rate of dry matter accumulation. Elevated CO_2 concentrations could increase the canopy temperature by keeping stomata closed with a decreasing transpiration rate (Yoshimoto et al., 2005), which would improve the photosynthetic efficiency of C3 species (e.g., rice, wheat) in particular, and be more likely to have increased yields than C4 species (Parry et al., 2004). Our results indicated that CO_2 fertilization effects would predominate over the effects of climate change in the middle and late 21st century, with benefits for rice yields. This is consistent with some previous studies in which increased temperatures would reduce crop yields but the fertilization effect of rising CO_2 concentration would offset the losses (Long et al., 2006; Tao et al., 2008a; Craufurd and Wheeler, 2009; Yu et al., 2014). Sun et al. (2009) quantified the yield increase of C3 crops to be 18% on average, ranging from 3% to 35% when CO_2 concentration increased from 300 ppm to 500–570 ppm in various free-air CO_2 enrichment (FACE) experiments. Our regression analysis obtained a similar response of yield to CO_2 fertilization, wherein rice yield increased 2.8% to 6.4% when CO_2 concentration increased by 100 ppm.

Without consideration of CO_2 effects, impacts of climate change on rice yield were positive for most stations in the NECP in the three future time periods under RCP4.5, and in the near term in RCP8.5 but negative toward the end of century. With consideration of CO_2 effects, yield in the NECP would increase significantly in the future, and high latitude areas would have a larger increase in yield than low latitude regions. Recent statistical analysis indicates that the rice planting area has been expanded in the NECP because of global climate change (Yang et al., 2015). However, variation in the size of yield increases would be greater in the second half of the century. To better adapt elevated CO_2 concentration, Shimono et al. (2009) noted selecting rice cultivars that enhancing magnitude of growth before heading is beneficial.

4.4. Uncertainty and limitations of the study

Different climate change projections may generate different results. To establish the range of uncertainty of climate projection, we used as many climate models as possible and assumed that all projections were feasible. Despite this, there were still uncertainties in the crop simulation model (Lobell et al., 2006; Tao et al., 2018). Although CERES-Rice has been widely used for climate change assessment studies globally, a single crop model is likely overconfident, which omits the uncertainty of crop model structure and parameters to the changing climate (Zhang et al., 2017; Tao et al., 2018). Multi-model ensembles are generally considered superior to single models in terms of increased reliability. This is because multi-model ensembles provide overall information from all participating models (Zhang et al., 2017). At present, assessments of yield response to future climate rely on climate and crop model (Challinor et al., 2013; Maiorano et al., 2017); therefore, refining model structure, optimizing parameters, and selecting the crop model suitable for research purposes should be taken into account.

Some other limitations of our simulations need to be discussed. Selecting only nine sites does not sufficiently capture the large climate variation across the NECP. For example, there is a great yield difference between northern and southern regions of NECP, which may be caused by different soil types and differences in water and nutrient assimilated by different cultivars. Therefore, our future work should provide a more detailed and comprehensive regional analysis at high resolution, which will generate a better understanding of the response of rice to future climate change in northeastern China. In addition, although CERES-Rice has well simulated the effects of climate change on rice growth and development and the responses of rice yield to various agricultural management practices, the current model does not sufficiently take into account yield reduction due to diseases, pests, weeds, and extreme weather events (e.g., floods, droughts, and extreme heat).

5. Conclusions

The CERES-Rice crop model has been well calibrated in the NECP. Statistical downscaling of climate data projected a small increase in radiation with large variability among 28 GCMs. Nevertheless, all GCMs consistently predicted increased temperature at the nine stations for both the RCP4.5 and RCP8.5 scenarios. Impacts of climate change on rice yield in the 21st century were assessed by combining the CERES-Rice crop model and 28 CMIP5 GCMs under two RCP scenarios in the NECP. Our study showed that although the rice-growing season would be shortened by 2–5 weeks, the projected effect of climate change on rice yield would be generally positive in northeast China. This is because of increased radiation as well as elevated CO_2 concentration. However, the magnitude of yield change depends on location. Future climate change has notable potential benefits for rice productivity in northeast China. We expect that expansion of the growing area and increased rice yield will positively affect China's food security. However, in the present study, we did not consider the effects of climate variability such as heat stress on rice productivity. Therefore, incorporating some useful agricultural management practices into the crop model, for example, adjusting the planting date, changing irrigation patterns, and developing high thermal requirements and rice cultivars with high heat tolerance, might be effective ways to tackle future climate change.

Acknowledgments

The study was supported by the climate change special foundation of China Meteorological Administration (No. CCSF201801) and National Natural Science Foundation of China (No. 41705095).

References

Anwar, M.R., Liu, D.L., Farquharson, R., Macadam, I., Abadi, A., Finlayson, J., et al., 2015. Climate change impacts on phenology and yields of five broadacre crops at four climatologically distinct locations in Australia. Agric. Syst. 132, 133–144.

Asseng, S., Ewert, F., Martre, P., Rotter, R.P., Lobell, D.B., Cammarano, D., et al., 2015. Rising temperatures reduce global wheat production. Nat. Clim. Chang. 5, 143–147.

Bai, H., Tao, F., 2017. Sustainable intensification options to improve yield potential and eco-efficiency for rice-wheat rotation system in China. Field Crop Res. 211, 89–105.

Bai, H., Tao, F., Xiao, D., Liu, F., Zhang, H., 2016. Attribution of yield change for rice-wheat rotation system in China to climate change, cultivars and agronomic management in the past three decades. Clim. Chang. 135, 539–553.

Berg, A., de Noblet-Ducoudré, N., Sultan, B., Lengaigne, M., Guimberteau, M., 2013. Projections of climate change impacts on potential C4 crop productivity over tropical regions. Agric. For. Meteorol. 170, 89–102.

Challinor, A.J., Smith, M.S., Thornton, P., 2013. Use of agro-climate ensembles for quantifying uncertainty and informing adaptation. Agric. For. Meteorol. 170, 2–7.

Chen, Y., Wang, P., Zhang, Z., Tao, F., Wei, X., 2017. Rice yield development and the shrinking yield gaps in China, 1981–2008. Reg. Environ. Change 17 (8), 2397–2408.

Chen, X., Cui, Z., Fan, M., Vitousek, P., Zhao, M., Ma, W., et al., 2014. Producing more grain with lower environmental costs. Nature 514, 486–489.

Craufurd, P.Q., Wheeler, T.R., 2009. Climate change and the flowering time of annual crops. J. Exp. Bot. 60, 2529–2539.

Cui, Z., Zhang, H., Chen, X., Zhang, C., Ma, W., Huang, C., et al., 2018. Pursuing sustainable productivity with millions of smallholder farmers. Nature 555, 363–366.

FAO, 2016. The State of Food and Agriculture 2016: Climate Change, Agriculture and Food Security (Rome).

FAO, 2018. http://www.fao.org/faostat/en/#data/QC.

FAO/IIASA/ISRIC/ISS-CAS/JRC, 2012. Harmonized World Soil Database (Version 1.2). FAO and IIASA, Rome, Italy and Laxenburg, Austria.

Guo, Y., Li, S., Liu, D.L., Chen, D., Williams, G., Tong, S., 2016. Projecting future temperature-related mortality in three largest Australian cities. Environ. Pollut. 208, 66–73.

He, Q., Zhou, G., 2016. Climate-associated distribution of summer maize in China from 1961 to 2010. Agric. Ecosyst. Environ. 232, 326–335.

He, L., Cleverly, J., Wang, B., Jin, N., Mi, C., Liu, D.L., et al., 2018. Multi-model ensemble projections of future extreme heat stress on rice across southern China. Theor. Appl. Climatol. 133, 1107–1118.

Hoogenboom, G., Porter, C.H., Shelia, V., Boote, K.J., Singh, U., White, J.W., et al., 2017. Decision Support System for Agrotechnology Transfer (DSSAT) Version 4.7. https://DSSAT.net DSSAT Foundation, Gainesville, Florida, USA.

IPCC, 2001. In: Houghton, J.T., Ding, Y., Griggs, D.J., Noguer, M., van der Linden, P.J., Dai, X., Maskell, K., Johnson, C.A. (Eds.), Climate Change 2001: The Scientific Basis. Contribution of Working Group I to the Third Assessment Report of the Intergovernmental Panel on Climate Change. Cambridge University Press, Cambridge, United Kingdom and New York, NY, USA (881 pp.).

IPCC, 2014. In: Field, C.B., Barros, V.R., Dokken, D.J., Mach, K.J., Mastrandrea, M.D., Bilir, T.E., Chatterjee, M., Ebi, K.L., Estrada, Y.O., Genova, R.C., Girma, B., Kissel, E.S., Levy, A.N., MacCracken, S., Mastrandrea, P.R., White, L.L. (Eds.), Climate Change 2014: Impacts, Adaptation, and Vulnerability. Part A: Global and Sectoral Aspects. Contribution of Working Group II to the Fifth Assessment Report of the Intergovernmental Panel on Climate Change. Cambridge University Press, Cambridge, United Kingdom and New York, NY, USA.

Jones, J.W., Hoogenboom, G., Porter, C.H., Boote, K.J., Batchelor, W.D., Hunt, L.A., et al., 2003. The DSSAT cropping system model. Eur. J. Agron. 18, 235–265.

Kim, H.Y., Ko, J., Kang, S., Tenhunen, J., 2013. Impacts of climate change on paddy rice yield in a temperate climate. Glob. Chang. Biol. 19, 548–562.

Laux, P., Jäckel, G., Tingem, R.M., Kunstmann, H., 2010. Impact of climate change on agricultural productivity under rainfed conditions in Cameroon—a method to improve attainable crop yields by planting date adaptations. Agric. For. Meteorol. 150, 1258–1271.

Lesk, C., Rowhani, P., Ramankutty, N., 2016. Influence of extreme weather disasters on global crop production. Nature 529, 84–87.

Liu, D.L., Zuo, H., 2012. Statistical downscaling of daily climate variables for climate change impact assessment over New South Wales, Australia. Clim. Chang. 115, 629–666.

Liu, Z., Li, Z., Tang, P., Li, Z., Wu, W., Yang, P., et al., 2013. Change analysis of rice area and production in China during the past three decades. J. Geogr. Sci. 23, 1005–1018.

Liu, Z., Yang, P., Tang, H., Wu, W., Zhang, L., Yu, Q., et al., 2014. Shifts in the extent and location of rice cropping areas match the climate change pattern in China during 1980–2010. Reg. Environ. Chang. 15, 919–929.

Liu, D.L., Zeleke, K.T., Wang, B., Macadam, I., Scott, F., Martin, R.J., 2017. Crop residue incorporation can mitigate negative climate change impacts on crop yield and improve water use efficiency in a semiarid environment. Eur. J. Agron. 85, 51–68.

Lobell, D.B., Gourdji, S.M., 2012. The influence of climate change on global crop productivity. Plant Physiol. 160, 1686–1697.

Lobell, D.B., Field, C.B., Cahill, K.N., Bonfils, C., 2006. Impacts of future climate change on California perennial crop yields: model projections with climate and crop uncertainties. Agric. For. Meteorol. 141, 208–218.

Long, S.P., Ainsworth, E.A., Leakey, A.D.B., Nosberger, J., Ort, D.R., 2006. Food for thought: lower-than-expected crop yield stimulation with rising CO_2 concentrations. Science 312, 1918–1921.

Maiorano, A., Martre, P., Asseng, S., Ewert, F., Müller, C., Rötter, R.P., et al., 2017. Crop model improvement reduces the uncertainty of the response to temperature of multi-model ensembles. Field Crop Res. 202, 5–20.

Parry, M.L., Rosenzweig, C., Iglesias, A., Livermore, M., Fischer, G., 2004. Effects of climate change on global food production under SRES emissions and socio-economic scenarios. Glob. Environ. Chang. 14, 53–67.

Piao, S., Ciais, P., Huang, Y., Shen, Z., Peng, S., Li, J., et al., 2010. The impacts of climate change on water resources and agriculture in China. Nature 467, 43–51.

Prudhomme, C., Reynard, N., Crooks, S., 2002. Downscaling of global climate models for flood frequency analysis: where are we now? Hydrol. Process. 16, 1137–1150.

Rosenzweig, C., Elliott, J., Deryng, D., Ruane, A.C., Muller, C., Arneth, A., et al., 2014. Assessing agricultural risks of climate change in the 21st century in a global gridded crop model intercomparison. Proc. Natl. Acad. Sci. U. S. A. 111, 3268–3273.

Ruane, A.C., McDermid, S., Rosenzweig, C., Baigorria, G.A., Jones, J.W., Romero, C.C., et al., 2014. Carbon-temperature-water change analysis for peanut production under climate change: a prototype for the AgMIP Coordinated Climate-Crop Modeling Project (C3MP). Glob. Chang. Biol. 20, 394–407.

Shi, X.Z., Yu, D.S., Warner, E.D., Pan, X.Z., Petersen, G.W., Gong, Z.G., et al., 2004. Soil database of 1:1,000,000 digital soil survey and reference system of the Chinese genetic soil classification system. Soil Surv. Horiz. 45, 129–136.

Shi, W., Tao, F., Liu, J., Xu, X., Kuang, W., Dong, J., et al., 2014. Has climate change driven spatio-temporal changes of cropland in northern China since the 1970s? Clim. Chang. 124, 163–177.

Shimono, H., Okada, M., Yamakawa, Y., Nakamura, H., Kobayashi, K., Hasegawa, T., 2009. Genotypic variation in rice yield enhancement by elevated CO_2 relates to growth before heading, and not to maturity group. J. Exp. Bot. 60, 523–532.

Sun, W., Huang, Y., 2011. Global warming over the period 1961–2008 did not increase high-temperature stress but did reduce low-temperature stress in irrigated rice across China. Agric. For. Meteorol. 151, 1193–1201.

Sun, J., Yang, L., Wang, Y., Ort, D.R., 2009. FACE-ing the global change: opportunities for improvement in photosynthetic radiation use efficiency and crop yield. Plant Sci. 177, 511–522.

Tao, F., Hayashi, Y., Zhang, Z., Sakamoto, T., Yokozawa, M., 2008a. Global warming, rice production, and water use in China: developing a probabilistic assessment. Agric. For. Meteorol. 148, 94–110.

Tao, F., Yokozawa, M., Liu, J., Zhang, Z., 2008b. Climate–crop yield relationships at provincial scales in China and the impacts of recent climate trends. Clim. Res. 38, 83–94.

Tao, F., Zhang, Z., Shi, W., Liu, Y., Xiao, D., Zhang, S., et al., 2013. Single rice growth period was prolonged by cultivars shifts, but yield was damaged by climate change during 1981–2009 in China, and late rice was just opposite. Glob. Chang. Biol. 19, 3200–3209.

Tao, F., Rotter, R.P., Palosuo, T., Diaz-Ambrona, C.G.H., Minguez, M.I., Semenov, M.A., et al., 2018. Contribution of crop model structure, parameters and climate projections to uncertainty in climate change impact assessments. Glob. Chang. Biol. 24, 1291–1307.

Tilman, D., Balzer, C., Hill, J., Befort, B.L., 2011. Global food demand and the sustainable intensification of agriculture. Proc. Natl. Acad. Sci. U. S. A. 108, 20260–20264.

Wang, W., Yu, Z., Zhang, W., Shao, Q., Zhang, Y., Luo, Y., et al., 2014. Responses of rice yield, irrigation water requirement and water use efficiency to climate change in China: historical simulation and future projections. Agric. Water Manag. 146, 249–261.

Wang, B., Liu, D.L., Macadam, I., Alexander, L.V., Abramowitz, G., Yu, Q., 2016. Multi-model ensemble projections of future extreme temperature change using a statistical downscaling method in south eastern Australia. Clim. Chang. 138, 85–98.

Wang, B., Liu, D.L., Asseng, S., Macadam, I., Yu, Q., 2017. Modelling wheat yield change under CO_2 increase, heat and water stress in relation to plant available water capacity in eastern Australia. Eur. J. Agron. 90, 152–161.

Wang, B., Liu, D.L., O'Leary, G.J., Asseng, S., Macadam, I., Lines-Kelly, R., et al., 2018. Australian wheat production expected to decrease by the late 21st century. Glob. Chang. Biol. 24, 2403–2415.

Willmott, C.J., 1982. Some comments on the evaluation of model performance. Bull. Am. Meteorol. Soc. 63, 1309–1313.

Wu, W., Fang, Q., Ge, Q., Zhou, M., Lin, Y., 2014. CERES-Rice model-based simulations of climate change impacts on rice yields and efficacy of adaptive options in Northeast China. Crop Pasture Sci. 65, 1267–1277.

Xiao, D., Tao, F., 2014. Contributions of cultivars, management and climate change to winter wheat yield in the North China Plain in the past three decades. Eur. J. Agron. 52, 112–122.

Xiong, W., Lin, E., Ju, H., Xu, Y., 2007. Climate change and critical thresholds in China's food security. Clim. Chang. 81, 205–221.

Xiong, W., Holman, I., Conway, D., Lin, E., Li, Y., 2008. A crop model cross calibration for use in regional climate impacts studies. Ecol. Model. 213, 365–380.

Xu, X.Z., Xu, Y., Chen, S.C., Xu, S.G., Zhang, H.W., 2010. Soil loss and conservation in the black soil region of Northeast China: a retrospective study. Environ. Sci. Pol. 13, 793–800.

Xu, Z., Shimizu, H., Yagasaki, Y., Ito, S., Zheng, Y., Zhou, G., 2013. Interactive effects of elevated CO_2, drought, and warming on plants. J. Plant Growth Regul. 32, 692–707.

Yang, Y., Yang, Y., Han, S., Macadam, I., Liu, D.L., 2014. Prediction of cotton yield and water demand under climate change and future adaptation measures. Agric. Water Manag. 144, 42–53.

Yang, X., Chen, F., Lin, X., Liu, Z., Zhang, H., Zhao, J., et al., 2015. Potential benefits of climate change for crop productivity in China. Agric. For. Meteorol. 208, 76–84.

Yoshimoto, M., Oue, H., Kobayashi, K., 2005. Energy balance and water use efficiency of rice canopies under free-air CO_2 enrichment. Agric. For. Meteorol. 133, 226–246.

Yu, Y., Zhang, W., Huang, Y., 2014. Impact assessment of climate change, carbon dioxide fertilization and constant growing season on rice yields in China. Clim. Chang. 124, 763–775.

Yun, J.I., 2003. Predicting regional rice production in South Korea using spatial data and crop-growth modeling. Agric. Syst. 77, 23–38.

Zhang, S., Tao, F., Zhang, Z., 2017. Uncertainty from model structure is larger than that from model parameters in simulating rice phenology in China. Eur. J. Agron. 87, 30–39.